

# Study of freeze-out dynamics in STAR at RHIC Beam Energy Scan Program

**Sabita Das (for the STAR collaboration)**

Institute of physics, Bhubaneswar - 751005, INDIA  
Brookhaven National Laboratory, Upton, NY, 11973-5000, USA

E-mail: [sabita@rcf.rhic.bnl.gov](mailto:sabita@rcf.rhic.bnl.gov)

**Abstract.** The STAR detector at RHIC, due to its large uniform acceptance and excellent particle identification capabilities, has measured a variety of hadron species ( $\pi^\pm$ ,  $K^\pm$ ,  $p$ ,  $\bar{p}$ ,  $K_S^0$ ,  $\Lambda$ ,  $\bar{\Lambda}$ ,  $\Xi^-$ ,  $\Xi^+$ ) produced in Au+Au collisions at  $\sqrt{s_{NN}} = 7.7, 11.5, 27$  and  $39$  GeV. These data are part of the Beam Energy Scan (BES) program at RHIC and provide an opportunity to measure the yields and transverse momentum spectra ( $p_T$ ) of the particles produced in the collisions. The corresponding measurements allow to study the freeze-out properties and dynamics of heavy ion collisions. A statistical thermal model analysis of particle production in BES energies in both grand canonical and strangeness canonical ensembles, is used to extract the chemical freeze-out parameters. The  $p_T$  spectra, particle ratios, and the energy and centrality dependence of freeze-out parameters determined from the thermal fit of particle ratios are discussed.

## 1. Introduction

Relativistic heavy-ion collisions provide the opportunity to study strongly interacting nuclear matter at different thermodynamic conditions. Quantum Chromodynamics (QCD), a fundamental theory to describe the interactions of quarks and gluons, has anticipated the transition from hadronic matter to a new state of matter called Quark-Gluon Plasma (QGP) [1] phase at high temperature and high energy density ( $\approx 1$  GeV/fm<sup>3</sup>). The QCD phase diagram is characterized by the temperature (T) and the baryon chemical potential ( $\mu_B$ ) or the (net) baryon density ( $n_B$ ), and it contains the information about the phase boundary that separates the QGP and hadronic phases [2,3]. Finite temperature lattice QCD calculations [4] predict a cross-over from hadronic to QGP phase at vanishing baryon chemical potential and large T while several QCD-based calculations [5] show that at lower T and  $\mu_B$  a first-order phase transition may take place. The point in the QCD phase diagram, where the first order phase transition ends would be the QCD critical point [6]. The BES program at RHIC has been carried out with the specific aim to explore several features of QCD phase diagram such as to search for the phase boundaries and the location of QCD critical point by colliding nuclei at several center-of-mass energies. When heavy ions collide at ultra-relativistic energies, the state of the system at the time of the final interaction is reflected by the observed single particle spectra. The process of hadron decoupling from an interacting system is called freeze-out. Freeze-out are of two types - kinetic and chemical freeze-out. Chemical freeze-out occurs at a temperature ( $T_{ch}$ ) when inelastic collisions cease and the particle yields become fixed and thermal (kinetic) freeze-out occurs at a temperature ( $T_{kin}$ ) when elastic collisions cease and particle transverse



momenta spectra are fixed.

In this paper we discuss the identified transverse momentum spectra and particle ratios produced in Au+Au collisions at  $\sqrt{s_{NN}} = 27$  GeV. Similar measurements at other BES center-of-mass energies  $\sqrt{s_{NN}} = 7.7, 11.5,$  and  $39$  GeV are reported in [7]. Statistical thermal models, such as THERMUS [8] have been proven to be successful in describing the particle production in heavy-ion collisions [9, 10, 11]. Experimental particle ratios are used in a statistical thermal model in both grand canonical ensemble (GCE) and strangeness canonical ensemble (SCE) approach to extract various chemical freeze-out parameters such as chemical freeze-out temperature ( $T_{ch}$ ), baryon chemical potential ( $\mu_B$ ), strangeness chemical potential ( $\mu_S$ ) and strangeness saturation factor ( $\gamma_S$ ). In this study we have used mid-rapidity particle ratios that include measured yields for charged pions ( $\pi^\pm$ ), charged kaons ( $K^\pm$ ), protons ( $p, \bar{p}$ ),  $K_S^0$ , lambdas ( $\Lambda, \bar{\Lambda}$ ) and cascades ( $\Xi^-, \Xi^+$ ) [7, 12]. The energy and centrality dependence of extracted chemical freeze-out parameters in Au+Au collisions at above BES energies are studied.

## 2. Results

### 2.1. Identified particle spectra and ratios

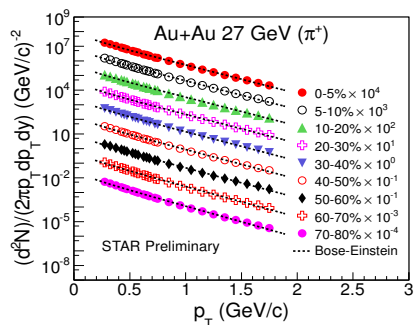


**Figure 1.** Transverse momentum spectra for charged pion at mid-rapidity ( $|y| < 0.1$ ) in Au+Au collisions at  $\sqrt{s_{NN}} = 27$  GeV. Errors shown here are statistical only. The lines represents the Bose-Einstein fits to the  $p_T$ -spectra.

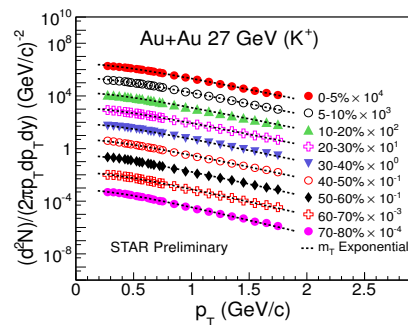


**Figure 2.** Transverse momentum spectra for charged kaon at mid-rapidity ( $|y| < 0.1$ ) in Au+Au collisions at  $\sqrt{s_{NN}} = 27$  GeV. Errors shown here are statistical only. The lines represents the  $m_T$  exponential fits to the  $p_T$ -spectra.

Figures 1 and 2 show the transverse momentum spectra of  $\pi^+$  and  $K^+$  respectively in Au+Au collisions at  $\sqrt{s_{NN}} = 27$  GeV in different centralities at mid-rapidity  $|y| < 0.1$ . The  $p_T$ -integrated pion yields obtained from the Bose-Einstein fit to  $p_T$ -spectra have been corrected for feed-down from weak decays. The  $m_T$ -exponential fit is used to obtain the  $p_T$ -integrated kaon yields. The collision-energy dependence of the anti-particle to particle ratios in central heavy-ion collisions for  $\pi^-/\pi^+$  and  $K^-/K^+$  are shown in Fig. 3. The  $\pi^-/\pi^+$  ratio at lower beam energies have values larger than unity, which could be due to significant contributions from resonance decays (such as from  $\Delta$  baryons). The  $\bar{p}/p$  ratio, not shown in this paper, increases with increasing collision energy and approaches unity for top RHIC energies [21]. This indicates that at higher beam energies, the  $p$  ( $\bar{p}$ ) production at mid-rapidity is dominated by pair production. The  $K^-/K^+$  ratio approaches unity as collision energy increases, indicating the dominance of kaon-pair production while at lower BES energies associated production of  $K^+$  dominates.

### 2.2. Chemical freeze-out

At chemical freeze-out, inelastic collisions among the particles stop and hadron yields are fixed. In Au+Au collisions at  $\sqrt{s_{NN}} = 27$  GeV, the measured mid-rapidity particle ratios including yields of  $\pi, K, p, K_S^0, \Lambda$  and  $\Xi$  are used in THERMUS. The thermal model fit of other BES

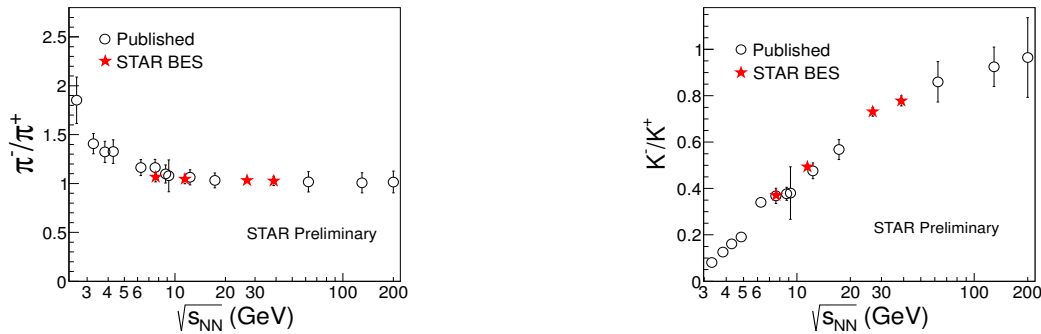


**Figure 3.**  $\pi^-/\pi^+$  and  $K^-/K^+$  ratios for 0–5% centrality in Au+Au collisions at  $\sqrt{s_{NN}} = 27$  GeV compared with the other BES energies and previous published results from AGS, SPS, and RHIC [14–22] respectively. Errors are the quadratic sum of statistical and systematic uncertainties.

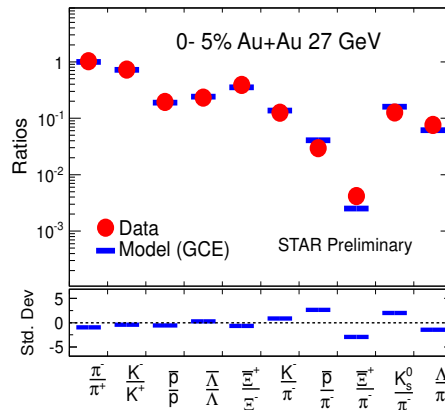


**Figure 4.** Statistical thermal model [8] fit to experimental mid-rapidity particle ratios using grand-canonical ensemble for 0–5% centrality in Au+Au at  $\sqrt{s_{NN}} = 27$  GeV.

energies at  $\sqrt{s_{NN}} = 7.7, 11.5,$  and  $39$  GeV is discussed in [13]. The  $\pi, K, p$  yields are measured at rapidity  $|y| < 0.1$  and those for  $K_S^0, \Lambda, \Xi$  are measured for  $|y| < 0.5$ . The errors on particle ratios including yields of  $\pi, K, p, K_S^0, \Lambda,$  and  $\Xi,$  are the quadratic sum of statistical and systematic uncertainties. Proton and anti-proton yields have not been corrected for feed-down contributions. The  $\Lambda$  yields have been corrected for the feed-down contributions from  $\Xi$  and  $\Xi^0$  weak decays [12]. The errors on freeze-out parameters are obtained from the THERMUS model and errors on particle ratios are treated as independent errors. Figure 4 shows the statistical thermal model fit to experimental particle ratios for 0–5% centrality in Au+Au collisions at  $\sqrt{s_{NN}} = 27$  GeV. The data show a good agreement with the fit to model having  $\chi^2/d.o.f = 23.8/6$ . Figure 5(a) shows that the  $T_{ch}$  increases with increasing collision energy. Figure 5(b) shows that the  $\mu_B$  decreases with increasing collision energy and it increases when going from peripheral to central collisions at lower energies. We observe a centrality dependence of chemical freeze-out curve ( $T_{ch}$  vs.  $\mu_B$ ) at BES energies which was not observed at higher energies of Au+Au 200 GeV [10].

In contrast to GCE approach where all quantum numbers are conserved on average, the THERMUS model also allows for a strangeness canonical ensemble where only the strangeness quantum number is required to be conserved exactly where as baryon and charge quantum numbers are conserved on an average. It is observed that in peripheral collisions,  $T_{ch}$  and  $\mu_B$

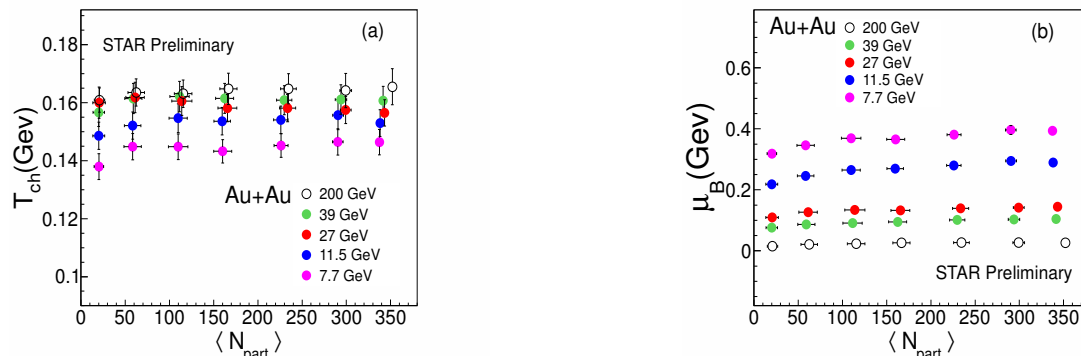


**Figure 5.** Results from a statistical thermal model fit [8] for Au+Au at  $\sqrt{s_{NN}} = 7.7, 11.5, 27$  and  $39$  GeV. Chemical freeze-out temperature, baryon chemical potential, and strangeness saturation factor are shown as a function of the average number of participating nucleons. The 200 GeV results are taken from Ref. [10].

follow a different behavior in GCE and SCE at lower BES energies [13]. Further studies by using the yields for the thermal fit towards a more quantitative analysis for all the BES energies are ongoing.

### 3. Conclusions

The study of the hadron particle ratios at BES energies in STAR within the framework of a statistical model yields the following conclusions. A centrality dependence of the chemical freeze-out parameters is observed at the lower energies. Baryon chemical potential ( $\mu_B$ ) range extends from 20 to 400 MeV in the QCD phase diagram in the new BES measurements at  $\sqrt{s_{NN}} = 7.7, 11.5, 27$  and  $39$  GeV. A detailed study using particle yields and different choices of ensembles in the statistical model is ongoing: this is expected to provide a better understanding of the freeze-out dynamics.

### References

- [1] Adams J *et al* (STAR Collaboration) 2005 *Nucl.Phys. A* **757** 102
- [2] Braun-Munzinger P *et al* 2011 *arXiv:1101.3167*
- [3] Mohanty B 2009 *Nucl. Phys. A* **830** 899C
- [4] Aoki Y *et al* 2006 *Nature* **443** 675
- [5] Ejiri S 2008 *Phys. Rev. D* **78** 074507; Bowman E S and Kapusta J I 2009 *Phys. Rev. C* **79** 015202
- [6] Gupta S *et al* 2011 *Science* **332** 1525
- [7] Kumar L (STAR Collaboration) 2011 *J. Phys. G Nucl. Part. Phys.* **38** 124145
- [8] Cleymans J *et al* 2009 *Computer Physics Communications* **180** 84
- [9] Cleymans J *et al* 2005 *Phys.Rev. C* **71** 054901
- [10] Aggarwal M M *et al* (STAR Collaboration) 2011 *Phys. Rev. C* **83** 024901; Kumar L (STAR Collaboration) 2013 *Nucl. Phys. A* **904-905** 256C
- [11] Cleymans J *et al* 2006 *Phys. Rev. C* **73** 034905
- [12] Zhu X (STAR Collaboration) 2012 *Acta Phys. Polon. B Proc. Supp.* **5** 213-218
- [13] Das S (STAR Collaboration) 2013 *Nucl. Phys. A* **904-905** 891C
- [14] Ahle L *et al* (E866 Collaboration and E917 Collaboration) 2000 *Phys. Lett. B* **490** 53
- [15] Klay J L *et al* (E895 Collaboration) 2002 *Phys. Rev. Lett.* **88** 102301
- [16] Ahle L *et al* (E866 Collaboration and E917 Collaboration) 2000 *Phys. Lett. B* **476** 1
- [17] Afanasiev S V *et al* (NA49 Collaboration) 2002 *Phys. Rev. C* **66** 054902
- [18] Alt C *et al* (NA49 Collaboration) 2008 *Phys. Rev. C* **77** 024903
- [19] Anticic T *et al* (NA49 Collaboration) 2004 *Phys.Rev. C* **69** 024902
- [20] Abelev B I *et al* (STAR Collaboration) 2009 *Phys. Rev. C* **79** 034909
- [21] Adams J *et al* (STAR Collaboration) 2004 *Phys. Rev. Lett.* **92** 112301
- [22] Abelev B I *et al* (STAR Collaboration) 2010 *Phys. Rev. C* **81** 024911